Superconductor Science and Technology

Description of hysteretic current–voltage characteristics of superconductor–normal metal–superconductor junctions

To cite this article: D M Gokhfeld 2006 *Supercond. Sci. Technol.* **20** 62

INSTITUTE OF PHYSICS PUBLISHING SUPERCONDUCTOR SCIENCE AND TECHNOLOGY
Supercond. Sci. Technol. **20** (2007) 62–66 doi:10.1088/0953-2048/20/1/011

Description of hysteretic current–voltage characteristics of superconductor–normal metal–superconductor junctions

D M Gokhfeld

L V Kirensky Institute of Physics, SD RAS, Krasnoyarsk, 660036, Russia

E-mail: gokhfeld@iph.krasn.ru

Received 21 September 2006, in final form 23 October 2006
Published 4 December 2006
Online at stacks.iop.org/SUST/20/62

Abstract
A simplified model for the current–voltage characteristics of weak links is suggested. It is based on an approach considering the multiple Andreev reflection in a metallic Josephson junction. The model allows one to calculate the current–voltage characteristics of superconductor–normal metal–superconductor junctions with different thicknesses of normal layer at different temperatures. A hysteretic peculiarity of the $V(I)$ dependence is described as a result of the negative differential resistance. The current–voltage characteristics of tin microbridges and high-T_c composite YBCO + $BaPbO_3$ were computed.

1. Introduction

Superconductor–normal metal–superconductor (SNS) junctions have current–voltage characteristics (CVCs) with rich peculiarities. Given certain parameters of the junctions, the CVCs of SNS junctions demonstrate excess current, subharmonic gap structure and negative differential resistance at low bias voltage. The region of negative differential resistance corresponds to the hysteresis of voltage in the bias current measurements. SNS junctions with nonlinear CVCs are promising for different applications, e.g. as low-noise mixers in the submillimetre-wave region [1, 2], switchers [3], and nanologic circuits [4].

The description of the CVCs of SNS junctions has been the subject of many articles, and the key role of multiple Andreev reflections has been recognized [5–10]. The main features of CVCs enumerated above are successfully described by the Kümmel–Gunsenheimer–Nicolsky theory (KGN) [7]. KGN theory is applicable for thick and clean weak links, where the normal metal layer N has a thickness $2a$ larger than the coherence length of the superconductor, and inelastic mean free path l larger than $2a$. A simplified model in the frame of KGN theory was developed by Pereira and Nicolsky [11]. This simple model is relevant for the weak links with thin superconducting banks S. The contribution of scattering states [7] is omitted in the model [11].

The Pereira–Nicolsky and KGN models were applied earlier to describe experimental CVCs of various weak links [12–17]. Experience of applications demonstrates that the oversimplified Pereira–Nicolsky model gives only a qualitative description. We suggest a new simple modification of KGN theory. It is shown that the CVCs of SNS junctions can be computed without all the complex ansatz of KGN theory. We hope this will lead to more extensive use of the KGN-based approach to the calculation of weak link characteristics.

2. Current–voltage characteristics

2.1. Model

Let us consider a voltage-biased SNS junction with a constant electric field which is in the negative z direction perpendicular to the NS interfaces and exists in the N layer only (figure 1). The normal layer has a thickness $2a$. The thickness of the superconducting bank is $D - a \gg 2a$.

The dynamics of quasiparticles in an SNS junction was considered in [7], where the time-dependent Bogoliubov–de Gennes equations are solved for the wave packets of nonequilibrium electrons and holes. The main result of [7] is the expression for dissipative current density in SNS junctions. For an SNS junction with thick superconducting banks ($D - a \gg 2a$), the dependence of current on voltage is deduced in [7] as

$$I(V) = \frac{e\hbar}{2am^*} \sum_{n=1}^{\infty} \exp\left(-\frac{2a}{l}n\right)$$

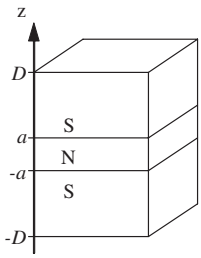

Figure 1. SNS junction.

$$\int_{-\Delta+neV}^{\Delta+eV} \mathrm{d}E \sum_r g_r(E) P_{\mathrm{N}}(E) k_{z\mathrm{F}} \tanh\left(\frac{E}{k_{\mathrm{B}}T}\right) + \frac{V}{R_{\mathrm{N}}}, \tag{1}$$

where $g_r(E)$ is the two-dimensional density of states, $P_{\mathrm{N}}(E)$ is the probability of finding of the quasiparticles with the energy E in the N region, m^* is the effective mass of an electron, l is the inelastic mean free path and R_{N} is the resistance of the N region with the thickness $2a$, Δ is the value of the energy gap of the superconductor at the temperature T, $k_{z\mathrm{F}}$ is the z-component of the Fermi wavevector of quasiparticles, and n is the number of Andreev reflections which quasiparticles undergo before they move out of the pair potential well.

The calculations of density of states [18] and probability of finding of the quasiparticles [7] in the N region are needed before being able to calculate the current (1). The probability $P_{\mathrm{N}}(E)$ of finding quasiparticles with energy E in the N region is given by equation (2.19) of [7]:

$$P_{\mathrm{N}}(E) = \frac{2a}{2a + 2\lambda} \tag{2}$$

with the penetration depth $\lambda = \frac{\hbar^2}{m^*} \frac{k_{z\mathrm{F}}}{\sqrt{\Delta^2 - E^2}}$ for $E < \Delta$, $\lambda < D - a$ and $\lambda = D - a$ otherwise. For quasiparticles from the scattering states, $P_{\mathrm{N}}(E) = 2a/2D$. Let us accept for the sake of simplicity that $\lambda \gg a$. Therefore $P_{\mathrm{N}}(E) = 2a/2\lambda$ for the bound states.

2.2. *Density of states*

The density of states [18] is found from

$$g_r(E) = \frac{A}{\pi} \sum_r k_{z\mathrm{F},r} \left| \frac{\mathrm{d}E}{\mathrm{d}k_{z\mathrm{F}}} \right|^{-1}_{k_{z\mathrm{F},r}}, \tag{3}$$

where A is the normal layer area, and $k_{z\mathrm{F},r}$ defines the value of $k_{z\mathrm{F}}$ for which $E_r = E$.

The energy spectrum $E(k_{z\mathrm{F}})$ consists of the spatially quantized bound states and the quasicontinuum scattering states. The energy eigenvalue equation for the spatially quantized bound Andreev states [7] is transcendental; it can only be calculated numerically, and the results are shown in figure 2:

$$E_r(k_{z\mathrm{F}}) = \frac{\hbar^2 k_{z\mathrm{F}}}{2am^*} \left(r\pi + \arccos\frac{E_r}{\Delta} \right), \tag{4}$$

where $r = 0, 1, 2, \ldots$.

Let us simplify equation (4). The expansion of $\arccos(E/\Delta)$ in (4) to a Taylor series $(\pi/2 - E/\Delta + \cdots)$ up to the second term and the subsequent expressing of $E(k_{z\mathrm{F}})$ are executed. Then we insert the correcting multiplier C for best fitting of equation (4).

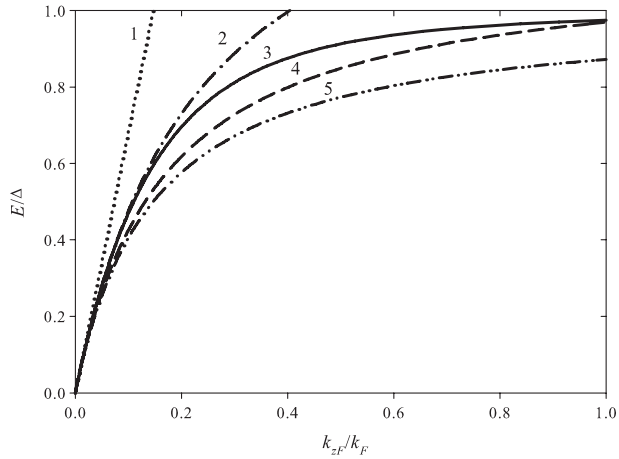

Figure 2. Energy of the bound Andreev state with $r = 0$; $2a = 5000$ Å; $\Delta = 0.57$ meV; $k_{\mathrm{F}} = 1.62$ Å^{-1}. (1) Equation (5), $C = 0$; (2) equation (5), $C = 1$; (3) the exact solution of equation (4); (4) equation (5), $C = \pi/2(1 - am^*\Delta/\hbar^2 k_{\mathrm{F}})$; (5) equation (5), $C = \pi/2$.

$$E_r(k_{z\mathrm{F}}) \approx \frac{\hbar^2 k_{z\mathrm{F}}}{2am^*} \pi \left(r + \frac{1}{2}\right) \Big/ \left(1 + C\frac{\hbar^2 k_{z\mathrm{F}}}{2am^*\Delta}\right). \tag{5}$$

If $C = 0$ then the spectrum of the Pereira–Nicolsky model is reproduced (curve 1, figure 2). Kümmel used equation (5) with $C = \pi/2$ [19] for approximate calculation of the energy spectrum (curve 5, figure 2).

The density of bound states follows from (3) and (5):

$$g_r(E) = \frac{A}{\pi} \left(\frac{2m^*a}{\hbar^2}\right)^2 \sum_r \frac{E}{\pi^2 \left(r + \frac{1}{2}\right)^2 \left(1 - C\frac{E}{\pi\left(r+\frac{1}{2}\right)\Delta}\right)^3}. \tag{6}$$

For quasiparticles from the quasicontinuum states, the energy spectrum is approximated by the continuous BCS spectrum of a homogeneous superconductor [7, 18]:

$$E(k_{z\mathrm{F}}) = \sqrt{\left(\frac{\hbar^2}{2m^*}\left(k_{\mathrm{F}}^2 - k_{z\mathrm{F}}^2\right)\right)^2 + \Delta^{*2}}. \tag{7}$$

For an SNS junction with thick superconducting banks, the effective energy gap Δ^* equals Δ. Then the density of quasicontinuum scattering states is

$$g(E) = \frac{A}{\pi^2} \frac{2m^*}{\hbar^2} k_{\mathrm{F}} D \frac{E}{\sqrt{E^2 - \Delta^2}}. \tag{8}$$

It is reasonable to choose the variable multiplier C from the best fitting of the energy spectrum and the density of states. We suggest that $C = \pi/2(1 - am^*\Delta/\hbar^2 k_{\mathrm{F}})$ for $C > 1$ and $C = 1$ otherwise. Such choice of C provides a good agreement of equation (5) (curve 4, figure 2) with the numerical solution of equation (4) for different relations of $a, m^*, \Delta, k_{\mathrm{F}}$. The coincidence of resulted density of states with $g(E)$ of [18] is satisfactory (figure 3).

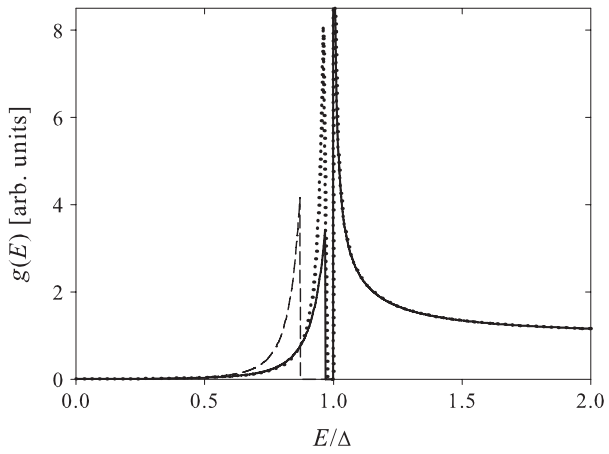

Figure 3. Density of states $g(E)$ of SNS junction with thick superconducting banks of [18] (dotted line), $g(E)$ calculated by equation (5) with $C = \pi/2$ (dashed line), $g(E)$ calculated by equation (5) with $C = \pi/2(1 - am^*\Delta/\hbar^2 k_F)$ (solid line). $D = 70\,000$ Å; $2a = 5000$ Å; $T_c = 3.77$ K; $k_F = 1.62$ Å^{-1}.

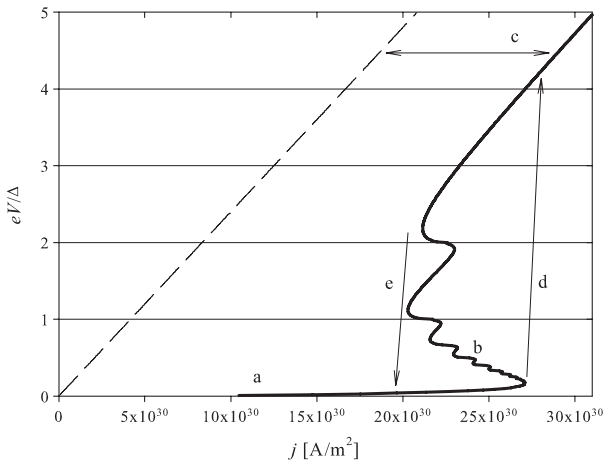

Figure 4. Voltage-biased current–voltage characteristic of SNS junction with steep rise of current (a), region of negative differential resistance (b), excess current density j_{ex} (c). $T_c = 3.77$ K, $\Delta_0 = 0.57$ meV, $k_F = 1.62$ Å^{-1}, $2a = 5000$ Å, $l = 15a$, $T = 0.1T_c$. Arrows (d) and (e) display the hysteretic jumps of voltage in the current-biased CVC.

2.3. Current density

The current density of quasiparticles from bound states is found from (1) and (6):

$$j_{bs}(V) = \frac{em^{*2}a^2}{2\pi^3\hbar^5}\sum_n \exp\left(-\frac{2a}{l}n\right) \times \int_{-\Delta+neV}^{\Delta} dE \sum_r \frac{|E|\sqrt{\Delta^2 - E^2}}{\left(r+\frac{1}{2}\right)\left(1 - C\frac{|E|}{\pi\Delta\left(r+\frac{1}{2}\right)}\right)^3} \times \tanh\left(\frac{E}{2k_BT}\right). \quad (9)$$

After substitution of (8) in (1) and the exclusion of small terms, we get the current density of quasiparticles from quasicontinuum states:

$$j_{ss}(V) = \frac{e}{4\pi^2\hbar}k_F^2\sum_n \exp\left(-\frac{2a}{l}n\right) \times \int_{E_1}^{\Delta+eV} dE \frac{E\tanh(E/2k_BT)}{\sqrt{E^2 - \Delta^2}}, \quad (10)$$

where $E_1 = -\Delta + neV$ for $-\Delta + neV \geqslant \Delta$ and $E_1 = \Delta$ otherwise.

The current densities (9) and (10) include the voltage dependence only within the integral limits.

If $eV \gg k_BT$, Δ the integral in (10) can be transformed and the excess current density is as follows:

$$j_{ex}(V) = \frac{e}{2\pi^2\hbar}k_F^2\Delta\tanh\left(\frac{eV}{2k_BT}\right)\exp\left(-\frac{2a}{l}\right). \quad (11)$$

This excess current density is the same as that obtained in KGN theory (equation (4.12) in [7]).

Note that the $j_{bs}(V)$ dependence changes negligibly if the second summation in (9) is interrupted at $r = 0$. Therefore we can write the expression for the total current density as follows:

$$j(V) = \sum_n \exp\left(-\frac{2a}{l}n\right)\left\{\frac{2em^{*2}a^2}{\pi^3\hbar^5}\int_{-\Delta+neV}^{\Delta} \times dE\frac{|E|\sqrt{\Delta^2 - E^2}}{\left(1 - C\frac{2|E|}{\pi\Delta}\right)^3}\tanh\left(\frac{E}{2k_BT}\right) + \frac{ek_F^2}{4\pi^2\hbar} \times \int_{E_1}^{\Delta+eV} dE\frac{E}{\sqrt{E^2 - \Delta^2}}\tanh\left(\frac{E}{2k_BT}\right)\right\} + \frac{V}{R_NA}. \quad (12)$$

$C = \pi/2(1 - am^*\Delta/\hbar^2 k_F)$ for $C > 1$ and $C = 1$ otherwise; $E_1 = -\Delta + neV$ for $-\Delta + neV \geqslant \Delta$ and $E_1 = \Delta$ otherwise.

Equation (1) includes the functions which should be numerically calculated before or during the processes of integration. This makes computation of the $I(V)$ dependences long and complicated. However, the expression (12) can be easily calculated. This simplified model allows one to calculate the CVCs of weak links with thick $D - a \gg 2a$ superconducting banks. It operates for different thicknesses of normal layer $2a < l$ and different temperatures lower than T_c. The curves calculated for the same parameters by (1) and (12) are nearly coincident.

3. Comparison with experimental current–voltage characteristics

The steep rise of current density at low voltage, the arches of the subharmonic gap structure (SGS), and the excess current are reproduced (figure 4) in the computed CVCs (12). Multiple Andreev reflection is the main reason for these peculiarities [7]. The position of the $(n-1)$th arch of the SGS is between V_n and V_{n+1}, where $V_n = 2\Delta/(n-1)e$, so the largest first arch is between Δ/e and $2\Delta/e$. Small peaks on the arches near V_n are caused by the subgap peak on $g(E)$.

The number of allowed Andreev reflections decreases with increasing bias voltage [7]. The current density due to Andreev reflections decreases correspondingly. In that time the ohmic current density increases as well as the voltage. A region of negative differential resistance appears in the CVC if the

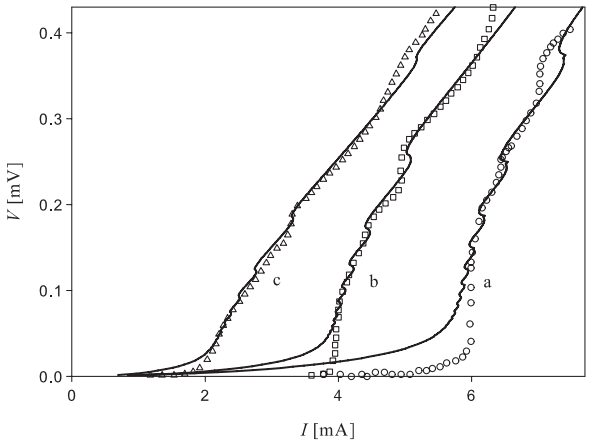

Figure 5. Current–voltage characteristics of tin microbridges. Experiments (points) and calculations (solid lines). Experimental $V(I)$ curves for (a) $T = 3.146$ K [22] and (b) $T = 3.5$ K, (c) $T = 3.633$ K [23].

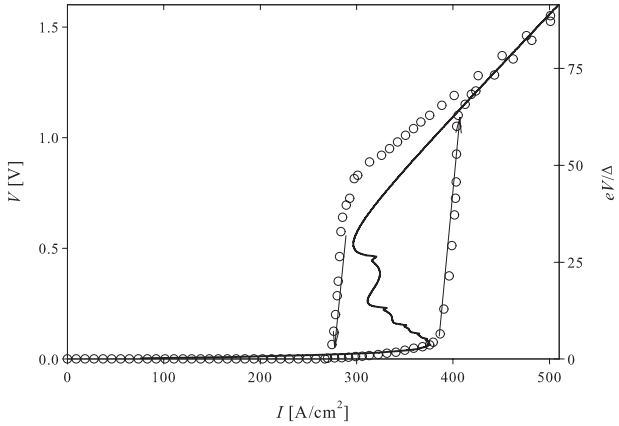

Figure 6. Current–voltage characteristic of composite YBCO + $BaPbO_3$ at $T = 4.2$ K. Experiment [13] (points) and calculation (solid line).

decrease of the Andreev current density is stronger than the increase of the ohmic current density. The measurement of the current-biased CVC demonstrates the hysteretic voltage jumps (figure 4) instead of the region of negative differential resistance.

To prove the model we first computed the CVCs of weak links made on a conventional superconductor (for details see [20]). We described the CVCs of tin microbridges [21–23] for different temperatures. The hysteretic peculiarity is absent in the CVCs. Figure 5 demonstrates the good pronounced arches of the SGS in the experimental and computed curves. Satisfactory agreement of the calculated curves and the experimental data is achieved [20] for the known parameters of Sn ($T_c = 3.77$ K, $\Delta_0 = 0.57$ meV, $k_F = 1.62$ Å^{-1}) and microbridges ($2a = 5000$ Å, $l = 15a$). Some discrepancy of the computed curves and the experimental points at low voltages is because in the experiments there were current-biased CVCs instead of voltage-biased ones.

Application of the model is also possible to describe the CVCs of a combination of weak links, e.g. networks and contacts connected in series. The networks of weak links, which occur in the polycrystalline high-T_c superconductors, have composite CVCs. These CVCs are a superposition of individual CVCs of the single weak links that constitute the network. Fitting parameters for current and voltage should be used in the model to account for a straining of the CVC along the I and V axes [11, 13]. Weak links connected in series (SNSNS...) can be realized in break junctions and wires with phase slip centres. In this case, the straining of CVCs along the V axis is accounted for by the formula for a series of weak links with dispersion of parameters [14–16]. The application of the model to the experimental CVCs of break junctions will be described in another article.

Here we use the developed model to compute the CVC of composite 92.5% YBCO + 7.5% $BaPbO_3$ [13]. Such a composite is a network of weak links. The experimental $V(I)$ curve at $T = 4.2$ K was fully reproducible for any velocity of current scanning. This is evidence that the hysteretic peculiarity in the CVC is not the result of self-heating. The $I(V)$ curve was computed for parameters of YBCO ($T_c =$ 93.5 K, $\Delta_0 = 17.5$ meV, $k_F = 0.65$ Å^{-1}, $m^* = 4m_e$). We set $l = 220$ Å, which is the value for the mean free path in $BaPbO_3$ [13]. A satisfactory agreement with the experimental $V(I)$ dependence was achieved for the parameter $2a = 50$ Å ($l = 9a$) (figure 6). This value of $2a$ coincides with the earlier estimations [13, 24]. The scale of the right-hand axis in units eV/Δ in figure 6 demonstrates the straining of the CVC due to the superposition of individual CVCs of single weak links.

4. Conclusion

A simplified model for the calculation of current–voltage characteristics of SNS junctions was developed. The KGN approach [7] was changed to be more convenient for a description of experimental CVCs of weak links with thick superconducting banks. The model operates for different thicknesses of normal layer $2a < l$ and different temperatures lower than T_c. The frequent observed peculiarities (steep rise of current, arches of subharmonic gap structure, negative differential resistance, excess current) in CVCs of SNS junctions are interpreted to be produced by multiple Andreev reflections. The hysteretic peculiarity is described as a result of the negative differential resistance.

It is demonstrated that the simplified model is useful for the quantitative description of CVCs of low- and high-T_c SNS junctions. The model was applied to compute the $V(I)$ dependences of tin microbridges and the hysteretic current–voltage characteristic of the high-T_c composite YBCO + $BaPbO_3$.

Acknowledgments

I am thankful to D A Balaev, R Kümmel and M I Petrov for fruitful discussions. This work is supported by a programme of the President of the Russian Federation for the support of young scientists (grant MK 7414.2006.2), Krasnoyarsk Regional Scientific Foundation (grant 16G065), a programme of the presidium of the Russian Academy of Science 'Quantum macrophysics' 3.4, and the Lavrent'ev competition of young scientist projects (project 52).

References

[1] Gorelov Y A, Pereira L A A, Luiz A M and Nicolsky R 1997 *Physica* C **282–287** 2491
[2] Matsui T and Ohta H 1999 *Supercond. Sci. Technol.* **12** 859
[3] Mamalis A G, Gokhfeld D M, Militsyn S V, Petrov M I, Balaev D A, Shaihutdinov K A, Ovchinnikov S G, Kirko V I and Vottea I N 2005 *J. Mater. Process. Technol.* **161** 42
[4] Hu C H, Jiang J F and Cai Q Y 2002 *Supercond. Sci. Technol.* **15** 330
[5] Klapwijk T M, Blonder G E and Tinkham M 1982 *Physica* B **109/110** 1657
[6] Flensberg K, Bindslev Hansen J and Octavio M 1988 *Phys. Rev.* B **38** 8707
[7] Kümmel R, Gunsenheimer U and Nicolsky R 1990 *Phys. Rev.* B **42** 3992
[8] Gunsenheimer U and Zaikin A D 1994 *Phys. Rev.* B **50** 6317
[9] Bratus' E N, Shumeiko V S, Bezuglyi E V and Wendin G 1997 *Phys. Rev.* B **55** 12666
[10] Bardas A and Averin D 1997 *Phys. Rev.* B **56** 8518
[11] Pereira L A A and Nicolsky R 1997 *Physica* C **282–287** 2411
[12] Pereira L A A, Luiz A M and Nicolsky R 1997 *Physica* C **282–287** 1529
[13] Petrov M I, Balaev D A, Gohfeld D M, Ospishchev S V, Shaihutdinov K A and Aleksandrov K S 1999 *Physica* C **314** 51
[14] Petrov M I, Balaev D A, Gokhfeld D M, Shaikhutdinov K A and Aleksandrov K S 2002 *Phys. Solid State* **44** 1229
[15] Petrov M I, Balaev D A, Gokhfeld D M and Shaikhutdinov K A 2003 *Phys. Solid State* **45** 1219
[16] Petrov M I, Gokhfeld D M, Balaev D A, Shaihutdinov K A and Kümmel R 2004 *Physica* C **408** 620
[17] Gokhfeld D M, Balaev D A, Shaykhutdinov K A, Popkov S I and Petrov M I 2006 *Phys. Met. Metallogr.* **101** (Suppl. 1) S27
[18] Plehn H, Gunsenheimer U and Kümmel R 1991 *J. Low Temp. Phys.* **83** 71
[19] Kümmel R 2004 private communications
[20] Gokhfeld D M 2006 *Preprint* cond-mat/0605427
[21] Gubankov V N, Kosheletz V P and Ovsyannikov G A 1977 *Sov. Phys. JETP* **73** 1435
[22] Octavio M, Skocpol W J and Tinkham M 1978 *Phys. Rev.* B **17** 159
[23] Gubankov V N, Kosheletz V P and Ovsyannikov G A 1981 *Fiz. Nizk. Temp.* **7** 277
[24] Petrov M I, Balaev D A, Ospishchev S V, Shaihutdinov K A, Khrustalev B P and Aleksandrov K S 1997 *Phys. Lett.* A **237** 85